Journal of Regenerative Medicine

Research Article

A SCITECHNOL JOURNAL

Zinc's Effect on the Differentiation of Porcine Adipose-derived Stem Cells into Osteoblasts

Josh Bertels[1], Marcello Rubessa[1], Mikhail E Kandel[2], Thomas Bane[1], Derek J Milner[1], Gabriel Popescu[2,3], and Matthew B Wheeler[1,3,4]*

Abstract

The aim of this project was to evaluate the effects of zinc in osteogenic media on differentiation of adipose-derived stem cells (ASC) into osteoblasts. ASC were plated (50,000 cells/mL) and subjected to treatments of zinc at six different concentrations in osteogenic medium: 8 mM, 4 mM, 0.8 mM, 0.4 mM, 0.08 mM, and 0.04 mM, as well as standard osteogenic medium as a positive control, and ASC culture medium as a negative control. At the end of the 4-week incubation period, cultures were analyzed for osteogenic differentiation, as measured by Alizarin Red S staining, osteocalcin production and Spatial Light Interference Microscopy (SLIM). Here we demonstrate that zinc supplementation to a standard ASC osteogenesis-promoting media formulation has a positive effect on the differentiation of porcine ASC into osteoblasts, and that 0.08 mM is the optimum concentration. Average size and number of osteogenic nodules increased under zinc supplementation, cells changed morphology more rapidly, and the concentration of osteocalcin released during osteogenic differentiation was higher ($p=0.0004$). Additionally we have demonstrated that a new non-invasive method utilizing SLIM microscopy can provide researchers another tool to probe intracellular and intracultural behavior *in vitro*, linking changes in cell behavior to differences in culture media formation. This specialized microscopic visualization technique may provide researchers with a good, non-invasive tool to evaluate the effect of molecular additives to media formulations on cell behavior, including potentially screening the effect of small molecule compounds derived from chemical libraries on cellular behavior *in vitro*.

Keywords

ASC; Stem cell; Zinc; Osteoblast

Introduction

Bone tissue is formed through the processes of endochondral or intramembranous ossification. During endochondral ossification, mesenchymal cells differentiate to form a cartilage template which is progressively converted into bone by invasion with stem cells that undergo osteogenesis and gradually convert the cartilaginous matrix to bone; while in intramembranous ossification mesenchymal stem cells (MSCs) differentiate directly into osteoblasts *in situ* to form bone [1]. Bone defects caused by natural degeneration or by traumatic injury place a significant burden on healthcare systems. In the US alone, there are approximately 6.2 million bone fractures annually [2]. While bone fractures typically heal well with monitoring and basic assistance by physicians, 10% of injuries will require bone grafting or other surgical intervention due to non-union healing, at a cost of approximately $2.5 billion annually [3,4]. Traditionally, these therapeutic methods to repair poor-healing injuries have included the use of autologous bone grafts, permanent metallic implants, or combinations of materials in order to repair bone defects sufficiently to restore proper function. While these therapeutic interventions frequently work well they can be taxing on the patient. Failure rates are still significant, and complications and revision surgeries to address failure of initial fracture healing treatments are common [5]. Factoring in patient morbidity, quality of life issues and lost work opportunity costs, total costs for these injuries swells to 4-6 times the amount for medical treatment. Orthopedic researchers have been continually engaged in devising and evaluating improved methods to treat severe bone injuries and poor-healing fractures. Recently, therapies utilizing MSCs have been put into practice in order to address a myriad of maladies arising in human medicine. While originally isolated from bone marrow, MSCs can be found residing in a number of different tissues. Adipose-derived stem cells (ASCs) are MSCs derived from fat tissue. Similar to their bone marrow-derived counterparts (BMSCs), ASCs are multipotent-able to differentiate towards osteogenic, adipogenic, myogenic, and chondrogenic lineages [6]. Compared to other tissues, adipose tissue represents an attractive source of stem cells due to the expendability of the tissue, relative safety of harvest, and increased concentration of stem cells harvested over other tissues such as muscle or bone marrow. Harvested ASCs are highly proliferative; flasks seeded with 3,500 ASCs are able to reach confluency in the same time frame as those seeded with 20,000-40,000 BMSCs, making them ideal for *in vivo* and *in vitro* experiments [7]. These cells are also attractive for potential bone repair therapies, as ASCs show robust mineralization within one week of *in vitro* osteogenic differentiation [5]. Working with the osteogenic potential of these stem cells, researchers have been able to repair bone defects in a wide range of animal models, showing the potential for ASCs to be integrated into a wide range of regenerative healing applications [8-10]. Zinc, a biological trace element, plays a critical role in cell and molecular physiology. It serves as an important cofactor for a number of proteins and enzymes. Zinc is essential for cell proliferation and differentiation; it is integral in the regulation of DNA synthesis and mitosis, can modulate cellular signal recognition, act to activate proteins, and it may stimulate or inhibit activities of transcription factors. Moreover, Zinc itself serves as an important cationic cofactor in a number of transcription factors [11]. Zinc has been shown to influence stem cell biology. Recent work has shown that zinc not only was required for embryonic development, but it also transiently maintained murine embryonic stem cell pluripotency [12]. Zinc plays an important role in bone metabolism and maintenance of bone health. Zinc deficiency decreases bone weight, delays bone growth and obstructs bone development [13]. Osteoporotic patients commonly show decreased levels of skeletal zinc [14,15]. Several studies have shown that Zinc promotes osteogenesis and bone matrix deposition in osteoblasts, while also inhibiting bone resorption by osteoclasts [16].

***Corresponding author:** Matthew B Wheeler, Professor of Biotechnology and Developmental Biology, Department of Animal Sciences, University of Illinois, 1207 West Gregory Drive, Urbana, IL 61801, USA, Tel: 217-333-2239; E-mail: mbwheele@illinois.edu

Received: April 04, 2019 **Accepted:** August 28, 2019 **Published:** September 04, 2019

Several zinc finger proteins have been shown to play important roles in stimulation of osteogenesis. The zinc finger protein 521 (Zfp521), also known as Early hematopoietic zinc finger (EHZF), is regarded as a crucial molecular regulator of the skeletal system [17,18]. During skeletal development, Zfp521 stimulates the maturation of osteoblasts during prenatal intramembranous bone formation [19]. The zinc finger protein Osterix, a downstream effector of Runx2, is expressed in all developing bones, and its activity is required for osteoblast differentiation. Meanwhile, the zinc finger protein TIZ has been shown to inhibit osteoclast genesis by modulating the activity of TRAF6 [16]. As with osteoblasts, osteogenesis of BMSCs has also been shown to be enhanced by the presence of zinc. BMSCs cultured on zinc coated titanium scaffolds and pushed toward osteogenesis show enhanced expression of osteogenic markers when compared to those cultured on bare titanium scaffolds [20]. Given that ASCs can readily undergo osteogenic differentiation, the aim of our study was to determine if exposure to increased levels of zinc can enhance the quality and extent of osteogenic differentiation in ASCs. Here we show that moderate amounts of increased zinc concentration enhance the formation of osteogenic nodules in ASC cultures, as measured by Alizarin Red S staining and SLIM interferometric microscopy.

Materials and Methods

Experimental design

ASC grown in culture differentiate into osteoblastic nodules that display accumulation of calcium deposits and bone matrix markers when cultured with osteogenic differentiation media [21]. The purpose of this work was to test if zinc had any effect on the osteogenic differentiation of ASC *in vitro*. To start this experiment, ASC were plated at a concentration of 50,000 cells/mL and subjected to treatments of zinc at six different concentrations in osteogenic medium: 8 mM, 4 mM, 0.8 mM, 0.4 mM, 0.08 mM, and 0.0 4mM, as well as standard osteogenic medium as a positive control, and ASC culture medium as a negative control. We used these concentrations because other papers have found the concentration of 0.4 mM to be non-toxic [22,23]. Cells were grown for 4 weeks in the appropriate media, with medium changed twice a week. At the end of the 4 week period, cultures were analyzed for osteogenic differentiation. Osteogenic differentiation was analyzed by three methods. First, osteogenic nodule formation was assayed by staining cultures with Alizarin Red S. With this stain, we determined whether any concentration of zinc had a positive effect on the formation of osteogenic nodules. In total, 3 biologically distinct replicates were grown and stained. Second, expression of the osteogenic marker osteocalcin was measured using a porcine osteocalcin enzyme-linked immunosorbent assay (ELISA) kit. This analysis was run to determine what the concentration of osteocalcin was in the medium at different zinc concentrations as well as the standard osteogenic medium. ELISA was run in duplicate on 5 samples to determine osteocalcin concentrations. Finally, spatial light interference microscopy (SLIM) was used to compare cell and nodule properties at different concentrations of zinc and in control media. 50,000 cells/mL were plated in a treated 6 well plate and grown, then imaged under the microscope between days 10-17, the point at which nodule formation begins [24]. This imaging method allowed us to measure cell mass, the advection speed velocity, and the diffusion coefficient of osteoblast formation. In total, 170 mosaic style images were acquired over a period of 145 hours using 12 terabytes of storage space.

ASC isolation and culture *in vitro*

Subcutaneous back fat and bone marrow were acquired from 3 castrated Yorkshire crossbred male pigs, at approximately 6 months of age, under protocols approved by the University of Illinois Institutional Animal Care and Use Committee (IACUC). Pigs were euthanized at the University of Illinois Meat Science Laboratory abattoir. The skin overlying the loin area was shaved to remove the hair and scrubbed three times using Betadine® solution (Povidoneiodine, 10%-Purdue Products L.P., Cranbury, NJ), and three times with 70% ethanol to avoid contamination of the sample. A square of subcutaneous back fat (~100 cm^2) was then excised from the sanitized area from each pig, placed in a sterile plastic bag, transported to the laboratory on ice and placed at 4°C until cell harvest (<1hr). The subcutaneous fat was dissected from the skin with a sterile scalpel. All the surfaces of the fat that were originally exposed at tissue harvest were also trimmed off with a sterile scalpel blade so the only sterile fat was processed for cell isolation. Strips of sterile fat were washed twice in Dulbecco's Phosphate Buffer Saline (DPBS, Sigma Aldrich D5773, St. Louis, MO) containing 1% Penicillin G-Streptomycin (Sigma P3539) and 5.0 mg/L of Amphotericin B (Sigma A9528). After washing, tissue was minced with scalpel blades and then digested with 0.075% collagenase type I-A (Sigma C2674) in DPBS, in a 50 ml conical tube (Corning, NY) (v/v-tissue/collagenase), in the incubator at 37°C for 90 min. The conical tubes, containing fat and collagenase, were vigorously shaken every 10 to 15 min to ensure a uniform digestion. After digestion, tubes were centrifuged at 200x g for 10 min at room temperature. The buoyant cell fraction and supernatant were discarded and 2 mL of red blood cell lysis buffer (Sigma R7757) was added to the pellet and gently mixed for 2 min. Subsequently, 20 mL of DPBS were added to the tubes and were centrifuged at 200x g for 5 min at room temperature, to obtain a cell pellet that was then re-suspended in culture medium. The culture medium used was high glucose Dulbecco's Modified Eagle's Medium (DMEM, Sigma D5648), supplemented with 10% Fetal Bovine Serum (FBS, BenchMark™, Gemini Bio-Products, West Sacramento, CA), plus 1% Penicillin G-Streptomycin and 5.0 mg/L of Amphotericin B. Cells were counted using an hemocytometer, plated in 75 cm^2 Corning cell culture flasks at 7.5×10^5 cells in 15 mL of culture medium, and incubated at 39°C and 5% CO_2 in 100% humidified air. Medium was changed every other day until the initial cell culture passage. Passage 0 cells reached confluence at approximately day 10 of culture. In order to keep the cells at a sufficiently low density to stimulate further growth, the initial cell cultures were washed using DPBS and harvested by digestion with 0.25% Trypsin (Sigma T4799)-0.04% EDTA (Sigma E6753) for 3 min. Trypsin was then inactivated by adding an equivalent volume of culture medium and the cells were centrifuged at 200x g for 5 min at room temperature. Cells were resuspended in culture medium for plating in 75 cm^2 cell culture flasks at a density of approximately 7.5×10^5 cells/75cm^2. These passage 1 cells were 80% confluent after 4 days. Cells were trypsinized, as described above, and frozen at 3×10^6 cells per 1.2 mL in cryogenic vials (Nalgene® Labware, Rochester, NY). Freezing medium consisted of 75% DMEM supplemented with 15% FBS and 10% dimethyl sulfoxide (DMSO, Sigma D2650). Vials were placed in Nalgene Cryo 1°C Freezing containers (Nalgene® Labware) and placed in a -80°C freezer. On the following day, cells were transferred to liquid nitrogen and stored until further use. Osteogenic medium used was made with 100 mL of high glucose Dulbecco's Modified Eagle's Medium (DMEM, Sigma D5648), 100 µL of Ascorbic acid-2-phosphate (Sigma 43752) at a concentration of 50 µg/mL, 1 mL of Beta Glycerophospate (10 mM), and 10 µL of Dexamethasone (100 nM). Once the media was complete, zinc sulfate heptahydrate ($ZnSO_4.7H_2O$) was added to give 6 concentrations: 8 mM, 4 mM, 0.8 mM, 0.4 mM, 0.08 mM, and 0.04 mM. These 6 treatments, along with a negative ASC culture medium control and a positive standard osteogenic medium control, were

plated at a concentration of 5×10^4 cells/mL of respective medium, and changed twice a week for a four-week period.

Alizarin Red S staining

Alizarin Red S staining has been used for decades to evaluate the presence of calcium-rich deposits formed by cells in culture. It is particularly versatile in that the dye can be extracted from the stained monolayer and assayed [25]. At the end of the four-week culture period, cells were washed with DPBS, and then fixed in 10% neutral buffered formalin for 30 min. Once fixed, cells were washed with ddH_2O and then stained with 2% Aliarin Red S, pH4.5 for 45 min. Alizarin Red S stain was removed, and stains were washed four times with ddH_2O, and then stored under DPBS. Red-stained nodules were then counted and evaluated on an Olympus inverted cell culture microscope and images were acquired using a Zeiss camera and running Zen software (Zeiss, Germany). Data were analyzed by analysis of variance using the Generalized Linear Model (GLM) procedure (SPSS 24-IBM). Bonferroni's post hoc test was used to perform statistical multiple comparison. The alpha level was set at 0.05.

Porcine osteocalcin ELISA

ELISA for porcine osteocalcin were perfomed using a porcine osteocalcin sandwich ELISA Kit (LifeSpan BioSciences Inc, LS-F5374). ELISA was performed according to the manufacturer protocol. A lyophilized standard was diluted as indicated and added to the first two lanes of the supplied 96-well Strip plate, pre-coated with a target specific capture antibodies. Thawed cell culture supernatants were centrifuged and added into the plate, then incubated at 37°C for 1 hour. Samples were aspirated off, then followed by a biotinylated detection antibody (diluted at a ratio of 1:100), followed by hour incubation at 37°C. The antibody solution was removed by aspiration and the plate was washed with a 1X wash buffer 3 times. An avidin-linked horseradish peroxidase solution (diluted at a ratio of 1:100) was added to the wells and incubated for 30 min at 37°C. This solution was then aspirated and the plate was washed 5 times with the 1X buffer, after which a TMB substrate was added to react with the peroxidase enzyme to provide colorimetric detection. Once color development reached its peak point, sulfuric acid was added to stop the reaction, and the plate was analyzed under a plate reader set to 450 nm. All recorded parameters were subjected to a Student-t Test. The alpha level was set at 0.05.

SLIM microscopy and time-lapse imaging

Time-lapse imaging was performed on an automated Zeiss microscope coupled to a SLIM interferometric add-on module (Phi Optics Inc.). This module enables us to acquire "phase-maps" that can readily be converted into measures of the cellular dry-mass [26]. The surface was treated with poly-d-lysine (PLD, Sigma-Aldrich) to promote cell attachment. Simultaneous time-lapse imaging was performed several hours after attachment (Figure 1). To automatically analyze the resulting data sets, we utilized a dynamic light scattering motivated technique termed "dispersion-relation phase spectroscopy" [DPS] [27]. This technique enables us to characterize the behavior changes associated with the differentiation process. Specifically, we use the transport of cellular dry-mass as a proxy for cellular activity at different size scales, notably those corresponding to small cellular structures associated with growth (for example, mitochondria, vesicles, etc) and larger cellular features such as the shape associated with cell type. Mosaic tiles were aligned and registered using the method outlined by Nguyen et al. [28]. As shown by Kandel et al. [28,29], the result of the Fourier projection is fit to a curve, with the first order term corresponding to the spread in advection (bulk flow) velocities and the second order term (if any) corresponding to diffusion. A 15-hour monitoring window was used to assign each time point an advection spread coefficient. This allows for the mass transport behavior to change through time, although in this work we observed no qualitative change between groups (see Results). The DPS calculation was performed in MATLAB using a large memory machine (196 GB of RAM), and thus the calculation is primarily limited by the speed of the hard disk array. We observed that the mass transport phenomena were primarily advective for all size scales and conditions, with the exception of large scale features at the start of the experiment for the ACS media condition. In that case, we observe a kind of diffusive transport phenomena not captured by

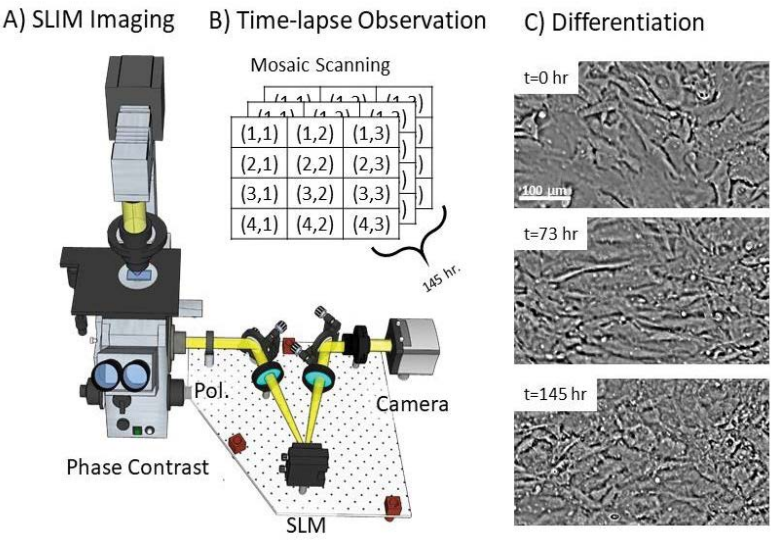

Figure 1: (A&B) Schematic representation of the SLIM interferometric add-on module (Phi Optics Inc.); (C) ASC timeline at different time points 0,73 and 145 hours.

our model, specifically at the start of the experiment the cells behave in a more disordered fashion resembling diffusive transport. The difference in behavior can be attributed to a comparably longer time to exit the lag phase of the growth cycle after plating.

Results

In vitro Alizarin Red S stain

Using methods established by Monaco et al. [21,24,30] and staining using Alizarin Red S, we were able to divide nodules into two groups: formed and forming nodules (Figure 2). The second evaluation performed was to evaluate the diameter of the largest nodules (2/well) in each group. The results showed that the doses of zinc of both 8 mM and 4 mM were toxic while the concentrations of 0.8 mM and 0.4 mM were not cytotoxic but no nodules formed. However, the 0.08 mM and 0.04 mM treatments showed positive effects on differentiation. In Table 1, results are summarized. Upon evaluating nodule diameter, we noted a trend between the zinc concentration and the diameter of the nodules. This difference can be explained by the results of Yamaguchi [15] that showed that there is a positive effect of the zinc on osteoblastic bone formation and the stimulation of the cellular synthesis. However, the differences in nodule size were not statistically significant (Figure 3).

ELISA measurement of osteocalcin expression

Using ELISA, we assayed osteocalcin levels in samples from the different treatments. We found a statistically significant difference in the level of osteocalcin produced in the cultures incubated with zinc compared to those in osteogenic media alone (T=4.0208; p=0.0004). This result suggested a better quality of the nodules formed in the osteogenic medium with zinc (Figure 4). Treatments are Zinc (0.08 mM) and Osteo (osteogenic control medium without supplemental zinc). Concentrations were determined by oprical density (OD) values at 450. ^{ab}The columns with different superscripts differ (p=0.0004, T=4.0208)

Time-lapse imaging

Finally, we used a dynamic light scattering derived technique [31], dispersion relation phase-spectroscopy [DPS] [27], to characterize the mass transport dynamics in live cell cultures undergoing osteogenesis. This technique reveals the spread in advection velocity of transport phenomena, enabling us to investigate cellular activity at a given spatial scale. Although dynamic light scattering has previously been used to distinguish between different cell types [32], and assay the trafficking of a limited number of differentiating cells (for example, [33]), to the best of our knowledge, this is the first time light scattering methods have been used for phenotypic, multi-well screening in a high-throughput manner. Significantly, such instrumentation has only recently become available [34]. As the qualitative differences between the four treatments remained constant for the duration of the imaging sequence, we summarize our findings in Figure 5. As a control, we include the ASC culture medium group (dashed) which exhibited neither diffusive nor adventive transport, as evidenced by the non-positive coefficient at t=0, at the scales in category 1 (see methods). As in previous studies with of long-term imaging and slower sampling rates [28] we did not observe diffusive transport behaviors. In line with our understanding that zinc promotes differentiation, size scales on the order of the cellular body (category 1) show an overall increase in mass transport (Table 2). Thus, cells treated with zinc appear to have a more rapidly changing morphology, as would be intuitively

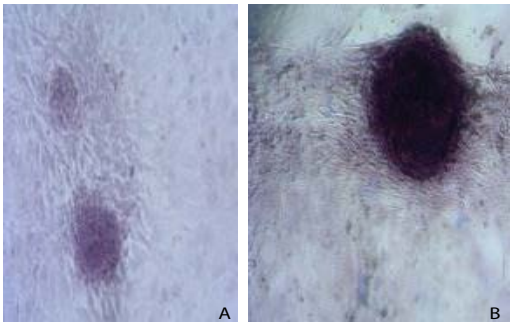

Figure 2: Forming *vs* formed nodule in 0.08 mM Zinc. Determination of forming nodule intensity set by Monaco [30]. The Figure A shows an example of forming nodules; in the Figure B an example of formed nodule.

Table 1: Number of formed and forming nodules per treatment.

Treatment	Formed Nodules	Forming Nodules	Total
0.08 mM Zinc	10.3 (3.1)^{a}	19.3 (4.2)^{A}	29.7 (6.4)^{Aa}
0.04 mM Zinc	9.3 (2.9)^{b}	7.3 (1.5)^{B}	16.7 (3.5)^{b}
Standard Osteogenic Medium	3 (0)^{c}	5.3 (1.1)^{B}	8.3 (1.1)^{Bb}
8 mM Zinc	0	0	0
4 mM Zinc	0	0	0
0.8 mM Zinc	0	0	0
0.4 mM Zinc	0	0	0
ASC Culture Medium	0	0	0

^{AB}Least square means (± SE) within each column without common superscripts differ significantly (p<0.01);

^{abc}Least square means (± SE) within each column without common superscripts differ significantly (p<0.05)

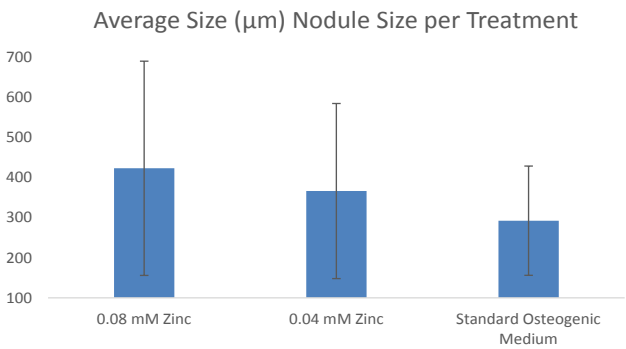

Figure 3: Average nodule size per treatment.

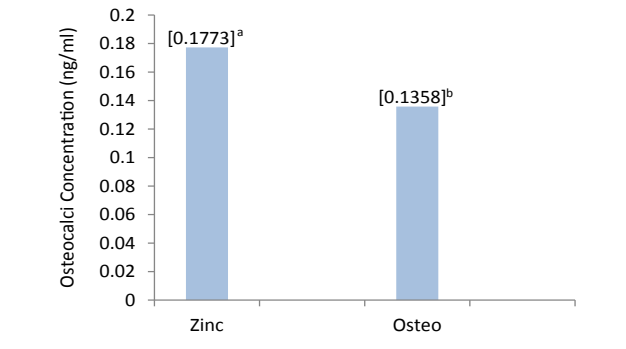

Figure 4: Average osteocalcin concentrations per treatment.

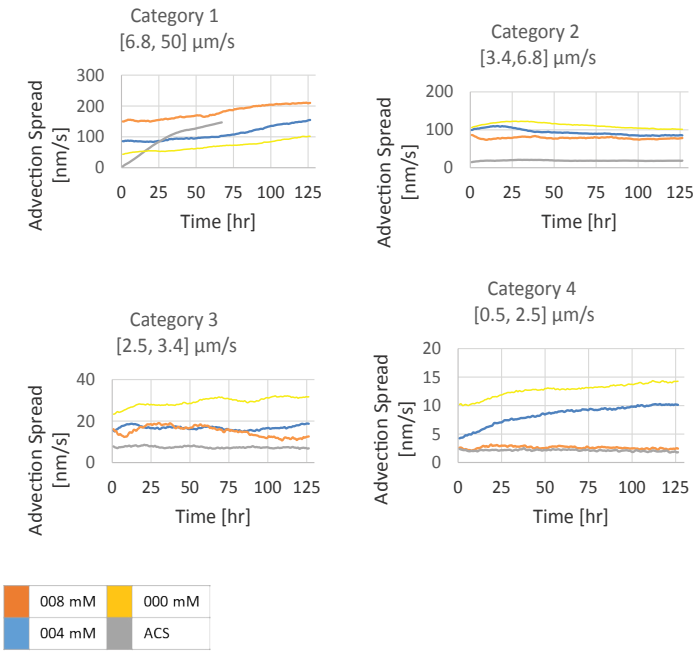

Figure 5: Stem cell behavior in the 4 treatment categories (categories is described in Table 1).

Table 2: Transport phenomena based on category.

Category	Scale [µm]	Transport Behavior in Ascending Order of Activity
1	6.75-50.0	0.08 mM 0.04 mM 0.00 mM (Standard Osteo) ASC culture medium*
2	3.4-6.75	0.00 mM (Standard Osteo) 0.04 mM 0.08 mM ASC culture medium
3	2.46-3.40	0.00 mM (Standard Osteo) 0.04 mM/0.08 mM ASC culture medium
4	0.55-2.46	0.00 mM (Standard Osteo) 0.04 mM 0.08 mM/ASC culture medium
*intersects lines /similar rates		

expected with increased differentiation rates. Interestingly, transport dynamics at finer size scales, such as those corresponding to cellular organelles display the opposite trend for mass transport (category 2, 3, 4). At those scales, corresponding to internal structures, zinc decreases transport activity, hinting at a metabolic trade-off between differentiation and an otherwise unmodified growth pattern. Thus cells that are actively differentiating (in zinc supplemented medium) have slower mass transport than undifferentiated cells that are growing (in control medium). This make perfect sense as growing and dividing cells are trying to produce more cellular organelles, replicate DNA, produce more cytoplasm and cell mass than differentiating cells whose metabolism has slowed during the differentiation process. In summary, with long-term imaging, we observe that the phenotypic differences in transport are a constant signature for the duration of the imaging period, with zinc increasing mass transport at size scales typically associated with cell bodies.

Discussion

Small variations in media composition by inclusion of bioactive additives can result in changes in cellular activity. This variation can be a change in one of the preexisting media components or the supplementation of a new one. These components can be hormones, sugars, minerals or other compounds, or they can be biologically complex mixtures such as serum or tissue extracts. Typically when deciding to introduce a new substance as a component of a culture media, the first step is to find the best concentration or a therapeutically-relevant range of concentration of the proposed additive, and then evaluate the results with respect to the cellular activity you are trying to enhance or improve. In this study we sought to evaluate the effect of zinc supplementation on osteogenic differentiation of ASC. The importance of the zinc for human physiology and homeostasis is well known, zinc is usually in the base formulations of several nutritional supplementations. Moreover, zinc has been shown to play an important role in bone development and health. Further, it has demonstrated effects on stem cell behavior as have other ions including iron and calcium [12,35]. Zinc plays an important role in several biological mechanisms, as it is a constituent of more than 200 enzymes involved in transcription, cell signaling and cell growth, differentiation and cancer [23,36-41]. For example, there are works demonstrating the effect of zinc deficiency on stem cell proliferation, leading to a direct correlation between zinc supplementation and cell proliferation [22, 39,41-43]. In this study we showed the positive impact of zinc supplementation on stem cell differentiation: the concentration of 0.08 Zn increased the formation of osteogenic nodules in differentiating ASC cultures (29.7 *vs* 8.3 Zn and standard osteogenic medium, respectively). These results are similar to findings reported where MSC were cultured with 2% zinc-glass [43]. Oh et al. demonstrated the positive effect of bioactive glass with zinc on osteogenesis of MSC cultures. In our study, comparing the best two zinc formulations and two standard media (ASC culture medium as a proliferation medium and the standard osteogenic

medium). We found an intermediate behavior when the zinc was present; the cells in osteogenic medium plus zinc had a behavior similar to the cells in DMEM: the mass transport in the cells treated with zinc is higher. These results confirmed the results obtained from other groups [44] showed how the zinc improved the cell mobility and restored the energetic metabolism in a toxic environment [22,44] showed the protective effect of the zinc [22]. Additionally, these results fall in line with what has been observed in previous experiments, focusing not only on the necessity of zinc for bone homeostasis, but also on its integral role in zinc finger protein 521 as a crucial regulator in the skeletal system and aid in the maturation of osteoblasts during prenatal intramembranous bone formation. These results also are not surprising, given that zinc has been shown to aid in the pluripotency of embryonic stem cells in mice.

Conclusion

We have shown that zinc supplementation to a standard ASC osteogenesis-promoting media formulation has a positive effect on the differentiation of porcine ASC into osteoblasts, and that 0.08 mM is the optimum concentration. Average size and number of osteogenic nodules increased under the influence of zinc, cells changed morphology more rapidly, and the concentration of osteocalcin released during osteogenic differentiation was statistically higher when the zinc was added at the osteogenic medium. We have shown the positive effect of the zinc addition to the osteogenic medium. This new formulation of culture medium could be used to study new drugs and their effects on bone formation. Further, these observations have led to new scaffold material formulations supplemented with zinc by our group. Additionally, we have demonstrated that a new non-invasive method utilizing light microscopy can provide researchers another tool to probe intracellular and intracultural behavior *in vitro*, linking changes in cell behavior to differences in culture media formation. This specialized microscopic visualization technique may provide researchers with a good, non-invasive tool to evaluate the effect of molecular additives to media formulations on cell behavior, including potentially screening the effect of small molecule compounds derived from chemical libraries on cellular behavior *in vitro*.

References

1. Shahi M, Peymani A, Sahmani M (2017) Regulation of Bone Metabolism. Rep Biochem Mol Biol 5: 73-82.
2. Bostrom MP, Saleh KJ, Einhorn TA (1999) Osteoinductive growth factors in preclinical fracture and long bone defects models. Orthop Clin North Am 30: 647-658.
3. Laurencin C, Khan Y, El-Amin SF (2006) Bone graft substitutes. Expert Rev Med Devices 3: 49-57.
4. Wu N, Lee Y, Segina D, Murray H, Wilcox T, et al. (2013) Economic burden of illness among US patients experiencing fracture nonunion. Orthopedic Research and Reviews 5: 21-33.
5. Levi B, James AW, Nelson ER, Vistnes D, Wu B, et al. (2010) Human adipose derived stromal cells heal critical size mouse calvarial defects. PloS one 5: e11177.
6. Zuk PA, Zhu M, Ashjian P, De Ugarte DA, Huang JI, et al. (2002) Human adipose tissue is a source of multipotent stem cells. Mol Biol Cell 13: 4279-4295.
7. Fraser JK, Wulur I, Alfonso Z, Hedrick MH (2006) Fat tissue: an underappreciated source of stem cells for biotechnology. Trends Biotechnol 24: 150-154.
8. Jing X, Yin W, Tian H, Chen M, Yao X, et al. (2018) Icariin doped bioactive glasses seeded with rat adipose-derived stem cells to promote bone repair via enhanced osteogenic and angiogenic activities. Life Sci 202: 52-60.
9. Lin CY, Wang YH, Li KC, Sung LY, Yeh CL, et al. (2015) Healing of massive segmental femoral bone defects in minipigs by allogenic ASCs engineered with FLPo/Frt-based baculovirus vectors. Biomaterials 50: 98-106.
10. Yoon E, Dhar S, Chun DE, Gharibjanian NA, Evans GR (2007) In vivo osteogenic potential of human adipose-derived stem cells/poly lactide-co-glycolic acid constructs for bone regeneration in a rat critical-sized calvarial defect model. Tissue Eng 13: 619-627.
11. Beyersmann D, Haase H (2001) Functions of zinc in signaling, proliferation and differentiation of mammalian cells. Biometals 14: 331-341.
12. Hu J, Yang Z, Wang J, Yu J, Guo J, et al. (2016) Zinc Chloride Transiently Maintains Mouse Embryonic Stem Cell Pluripotency by Activating Stat3 Signaling. PloS one 11: e0148994.
13. Seo HJ, Cho YE, Kim T, Shin HI, Kwun IS (2010) Zinc may increase bone formation through stimulating cell proliferation, alkaline phosphatase activity and collagen synthesis in osteoblastic MC3T3-E1 cells. Nutr Res Pract 4: 356-361.
14. Reginster JY, Strause LG, Saltman P, Franchimont P (1988) Trace elements and postmenopausal osteoporosis: a preliminary report of decreased serum manganese. Medical Science Research 16: 337-338.
15. Yamaguchi M (2010) Role of nutritional zinc in the prevention of osteoporosis. Mol Cell Biochem 338: 241-254.
16. Yamaguchi M (2012) Nutritional factors and bone homeostasis: synergistic effect with zinc and genistein in osteogenesis. Mol Cell Biochem 366: 201-221.
17. Xie XT, Zhan XL, Hu ZH (2017) [Zinc finger protein 521 suppresses osteogenic differentiation of rat mesenchymal stem cells by inhibiting the Wnt/beta-catenin signaling pathway]. Mol Biol (Mosk) 51: 464-472.
18. Hesse E, Kiviranta R, Wu M, Saito H, Yamana K, et al. (2010) Zinc finger protein 521, a new player in bone formation. Ann N Y Acad Sci 1192: 32-37.
19. Addison WN, Fu MM, Yang HX, Lin Z, Nagano K, et al. (2014) Direct transcriptional repression of Zfp423 by Zfp521 mediates a bone morphogenic protein-dependent osteoblast versus adipocyte lineage commitment switch. Mol Cell Biol 34: 3076-3085.
20. Gao CH, Li C, Wang CY, Qin YG, Wang ZH, et al. (2017) Advances in the induction of osteogenesis by zinc surface modification based on titanium alloy substrates for medical implants. J Alloy Compd 726: 1072-1084.
21. Monaco E, Bionaz M, Rodriguez-Zas S, Hurley WL, Wheeler MB (2012) Transcriptomics comparison between porcine adipose and bone marrow mesenchymal stem cells during in vitro osteogenic and adipogenic differentiation. PloS one 7: e32481.
22. Fathi E, Farahzadi R (2017) Zinc Sulphate Mediates the Stimulation of Cell Proliferation of Rat Adipose Tissue-Derived Mesenchymal Stem Cells Under High Intensity of EMF Exposure. Biol Trace Elem Res 184: 529-535.
23. Hasankolai MG, Batavani R, Eslaminejad MB, Gilani MS (2012) Effect of zinc ions on differentiation of bone marrow-derived mesenchymal stem cells to male germ cells and some germ cell-specific gene expression in rams. Biol Trace Elem Res 150: 137-146.
24. Kim D, Monaco E, Maki A, de Lima AS, Kong HJ, et al. (2010) Morphologic and transcriptomic comparison of adipose- and bone-marrow-derived porcine stem cells cultured in alginate hydrogels. Cell Tissue Res 341: 359-370.
25. Gregory CA, Gunn WG, Peister A, Prockop DJ (2004) An Alizarin red-based assay of mineralization by adherent cells in culture: comparison with cetylpyridinium chloride extraction. Anal Biochem 329: 77-84.
26. Mir M, Wang Z, Shen Z, Bednarz M, Bashir R, et al. (2011) Optical measurement of cycle-dependent cell growth. Proc Natl Acad Sci USA 108: 13124-13129.
27. Wang R, Wang Z, Millet L, Gillette MU, Levine AJ, et al. (2011) Dispersion-relation phase spectroscopy of intracellular transport. Optics Express 19: 20571-20579.
28. Nguyen TH, Kandel ME, Rubessa M, Wheeler MB, Popescu G (2017) Gradient light interference microscopy for 3D imaging of unlabeled specimens. Nature Communications 8: 210.
29. Kandel ME, Fernandes D, Taylor AM, Shakir H, Best-Popescu C, et al. (2017a) Three-dimensional intracellular transport in neuron bodies and neurites investigated by label-free dispersion-relation phase spectroscopy. Cytometry A 91: 519-526.

30. Monaco E, de Lima AS, Bionaz M, Maki A, Wilson SM, et al. (2009) Morphological and Transcriptomic Comparison of Adipose and Bone Marrow Derived Porcine Stem Cells. The Open Tissue Engineering and Regenerative Medicine Journal 2: 20-22.

31. Digman MA, Gratton E (2011) Lessons in Fluctuation Correlation Spectroscopy. Annu Rev Phys Chem 62: 645-668.

32. Kinnunen M, Karmenyan A (2015) Overview of single-cell elastic light scattering techniques. J Biomed Opt 20: 051040.

33. Takeda YS, Xu Q (2015) Neuronal Differentiation of Human Mesenchymal Stem Cells Using Exosomes Derived from Differentiating Neuronal Cells. PloS one 10: e0135111.

34. Kandel ME, Sridharan S, Liang J, Luo Z, Han K, et al. (2017b) Label-free tissue scanner for colorectal cancer screening. J Biomed Opt 22: 66016.

35. Webb SE, Miller AL (2003) Calcium signalling during embryonic development. Nat Rev Mol Cell Biol 4: 539-551.

36. Bafaro E, Liu Y, Xu Y, Dempski RE (2017) The emerging role of zinc transporters in cellular homeostasis and cancer. Signal Transduction And Targeted Therapy 2: 17029.

37. Bertels JC, Rubessa JC, Schreiber SR, Wheeler MB, (2016) 197 The effect of zinc on the differentiation of adipose-derived stem cells into osteoblasts. Reprod Fertil Dev 29: 207.

38. Foroutan T (2015) The effects of zinc oxide nanoparticles on differentiation of human mesenchymal stem cells to osteoblast. Nanomed J 1: 308-314.

39. Moon MY, Kim HJ, Choi BY, Sohn M, Chung TN, et al. (2018) Zinc Promotes Adipose-Derived Mesenchymal Stem Cell Proliferation and Differentiation towards a Neuronal Fate. Stem Cells Int 2018: 5736535.

40. Yamaguchi S, Miura C, Kikuchi K, Celino FT, Agusa T, et al. (2009) Zinc is an essential trace element for spermatogenesis. Proc Natl Acad Sci USA 106: 10859-10864.

41. Yusa K, Yamamoto O, Iino M, Takano H, Fukuda M, et al. (2016) Eluted zinc ions stimulate osteoblast differentiation and mineralization in human dental pulp stem cells for bone tissue engineering. Arch Oral Biol 71: 162-169.

42. Levenson CW, Morris D (2011) Zinc and neurogenesis: Making New Neurons from development to adulthood. Advances in Nutrition 2: 96-100.

43. Oh SA, Kim SH, Won JE, Kim JJ, Shin US, et al. (2011) Effects on growth and osteogenic differentiation of mesenchymal stem cells by the zinc-added sol-gel bioactive glass granules. J Tissue Eng 2010: 475260.

44. Yang X, Wang H, Huang C, He X, Xu W, et al. (2017) Zinc enhances the cellular energy supply to improve cell motility and restore impaired energetic metabolism in a toxic environment induced by OTA. Scientific Reports 7: 14669.

Author Affiliations

Top

[1]*Institute for Genomic Biology, University of Illinois, Urbana, IL, USA*

[2]*Department of Electrical and Computer Engineering, The University of Illinois at Urbana-Champaign, Urbana, IL, USA*

[3]*Department of Bioengineering, The University of Illinois at Urbana-Champaign, Urbana, IL, USA*

[4]*Department of Animal Sciences, University of Illinois, Urbana, IL, USA*